Published in final edited form as:
Dev Cell. 2009 March ; 16(3): 345–357. doi:10.1016/j.devcel.2009.01.022.

Nuclear export of Smad2 and Smad3 by RanBP3 facilitates termination of TGF-β signaling

Fangyan Dai[1,2,3], **Xia Lin**[2,3], **Chenbei Chang**[4], and **Xin-Hua Feng**[1,2,3,5]

1*Department of Molecular & Cellular Biology, Baylor College of Medicine, Houston, TX77030, USA*

2*Michael E. DeBakey Department of Surgery, Baylor College of Medicine, Houston, TX77030, USA*

3*The Dan L. Duncan Cancer Center, Baylor College of Medicine, Houston, TX77030, USA*

4*Department of Cell Biology, University of Alabama, Birmingham, AL35294, USA*

Summary

Smad2 and Smad3 (Smad2/3) are key intracellular signal transducers for TGF-β signaling and their transcriptional activities are controlled through reversible phosphorylation and nucleocytoplasmic shuttling. However, the precise mechanism underlying nuclear export of Smad2/3 remains elusive. Here we report the essential function of RanBP3 in selective nuclear export of Smad2/3 in the TGF-β pathway. RanBP3 directly recognizes dephosphorylated Smad2/3, which results from the activity of nuclear Smad phosphatases, and mediates nuclear export of Smad2/3 in a Ran-dependent manner. As a result, increased expression of RanBP3 inhibits TGF-β signaling in mammalian cells and *Xenopus* embryos. Conversely, depletion of RanBP3 expression or dominant negative inhibition of RanBP3 enhances TGFβ-induced anti-proliferative and transcriptional responses. In conclusion, our study supports a definitive role of RanBP3 in mediating Smad2/3 nuclear export and terminating TGF-β signaling.

Keywords

Smad; RanBP3; nucleocytoplasmic shuttling; signal transduction

Introduction

The transforming growth factor-beta (TGF-β) superfamily signaling controls a wide variety of biological processes from development to pathogenesis primarily through intracellular Smad proteins (Derynck and Miyazono, 2007). Smads are structurally and functionally grouped into three subfamilies: five receptor-activated Smads (R-Smads), one common Smad and two inhibitory Smads. Of R-Smads, Smad2 and Smad3 (Smad2/3 thereafter for simplicity) transduce activin and TGF-β signals, whereas Smad1, Smad5 and Smad8 transduce signals from the BMP/GDF (Bone Morphogenetic Proteins/Growth Differentiation Factor) family. Upon binding to their receptor complex at the cell surface, TGF-β and related growth factors activate Smad proteins and promote accumulation of Smads in the nucleus, where they mediate

5 To whom correspondence should be addressed: Department of Molecular & Cellular Biology, Baylor College of Medicine, One Baylor Plaza, Room R712, Houston, TX 77030, Phone: 713-798-4756, Fax: 713-798-4093, e-mail: E-mail: xfeng@bcm.edu.

transcriptional responses (ten Dijke and Hill, 2004; Massague et al., 2005; Feng and Derynck, 2005).

Smads possess intrinsic nucleocytoplasmic shuttling capacity and their subcellular distribution is determined through association with nuclear transport factors and retention proteins (Watanabe et al., 2000; Pierreux et al., 2000; Inman et al., 2002b; Nicolas et al., 2004; Schmierer and Hill, 2005). Although it has been reported that TGF-β-induced phosphorylation favors the nuclear import of phosphorylated R-Smads (P-Smads) by enhancing their association with importin-β (Xiao et al., 2000; Kurisaki et al., 2001) and/or disassociation with cytoplasmic retention factors such as SARA (Xu et al., 2000), live cell microscopy analysis suggest a pivotal role of nuclear export in regulating TGF-β signaling. TGF-β appears not to affect the nuclear import rate of Smad2 (Schmierer and Hill, 2005). Instead, it decreases Smad2 nuclear export, thereby retaining more the phosphorylated Smad2 in the nucleus (Xu et al., 2002; Schmierer and Hill, 2005). Conversely, dephosphorylation of P-Smad2/3 by phosphatase PPM1A promotes nuclear export of Smad2/3 (Lin et al., 2006). Therefore, the phosphorylation status of R-Smads is coupled with its nuclear accumulation (Xu et al., 2002; Inman et al., 2002b; Lin et al., 2006). It is generally thought that the level of nuclear R-Smads determines the duration and strength of signaling.

Unlike common Smad4 and BMP-specific Smad1, whose nuclear export depends on the function of CRM1, a Leptomycin B (LMB)-sensitive export receptor (Watanabe et al., 2000; Pierreux et al., 2000; Xiao et al., 2001; Xiao et al., 2003), TGF-β-specific Smad2/3 undergo nuclear export in a LMB-insensitive manner and appear to be independent of CRM1 function or Smad4 export (Pierreux et al., 2000; Inman et al., 2002b; Nicolas et al., 2004; Schmierer and Hill, 2005). It has been reported that TGF-β-specific Smad3 nuclear export involves TGF-β-dependent interaction with Exportin 4 (in the case of Smad3) (Kurisaki et al., 2006) and TGF-β independent interaction with nucleoporins (Xu et al., 2002). Given the highly conserved putative NESs and Exportin4-binding motifs between BMP- and TGF-β-specific R-Smads (Xiao et al., 2001; Kurisaki et al., 2006), it remains unresolved how export mediators discriminate these R-Smads.

In this study, we provide compelling evidence that Ran-binding protein 3 (RanBP3) serves as a direct mediator for nuclear export of Smad2/3. Originally identified as an interaction partner with the guanine nucleotide exchange factor (RCC1) (Mueller et al., 1998), RanBP3 has been implicated in the process of nucleocytoplasmic trafficking by its ability to bind a few proteins including Ran, nuclear pore components and CRM1 (Mueller et al., 1998; Englmeier et al., 2001; Lindsay et al., 2001). We found RanBP3 directly interacts with Smad2/3 in their dephosphorylated form, but not with Smad1. Consistent with its role in exporting Smad2/3, RanBP3 negatively regulates TGF-β signaling. Knockdown of RanBP3 or blockade of the RanBP3-Smad2/3 interaction inhibits Smad2 nuclear export and enhances TGF-β-induced responses. In accordance, RanBP3 represses activin/Smad2, but not BMP-Smad1 signaling in *Xenopus* embryos. These findings support the notion that nuclear export of R-Smads is selectively controlled by specific export mediators in the process of TGF-β signal termination.

Results

RanBP3 inhibits Smad2/3-mediated transcriptional responses in mammalian cells

In an attempt to identify novel intracellular factors controlling TGF-β signaling, we discovered that RanBP3 was a strong candidate for mediating nuclear export of Smad2/3. As a first step in evaluating a possible role of RanBP3 in TGF-β signaling, we examined the effects of RanBP3 on Smad2/3-mediated transcriptional activation using various Smad-dependent gene reporters. Increased expression of human or mouse RanBP3 caused a decrease in TGF-β-dependent transcription from the Smad-binding element (SBE)-Luc reporter (Figure 1A; data not shown).

RanBP3 also inhibited TGF-β-induced activation of the natural p21 promoter in HaCaT cells (Figure 1B), as well as the p15 promoter and the plasminogen activator inhibitor type 1 (PAI-1) promoter in HepG2 cells (data not shown). However, RanBP3-wv, a mutant that loses its Ran-binding activity (Englmeier et al., 2001), failed to block TGF-β-induced promoter activation, although the mutant was expressed at a similar level to that of RanBP3 (Figure 1C). In sharp contrast to its ability to regulate TGF-β signaling, RanBP3 did not interfere with BMP-induced activation of the Id1 promoter in C2C12 cells (Figure 1D) or HepG2 cells (Figure S3), suggesting that RanBP3 specifically acts on TGF-β, but not BMP, signaling.

Consistent with the ability of RanBP3 to inhibit activation of TGF-β-responsive promoters, HaCaT cells stably expressing RanBP3 (Figure 1H, blot a) diminished TGF-β-mediated induction of endogenous p15, p21 and PAI-1 mRNAs (Figure 1E-G). In addition, the protein level of p21 was also reduced (Figure 1H, blot b). Overexpression of RanBP3, however, did not disrupt the TGF-β-induced C-terminal phosphorylation of Smad2/3 (Figure 1H, blot c and d), nor did it affect the total level of Smad2/3 in the same stable cells (Figure 1H, blot e). These data suggest that RanBP3 acts downstream of Smad2/3 activation.

RanBP3 suppresses activin but not BMP signaling in *Xenopus* embryos

During early vertebrate development, activin/nodal and BMP signals are known to control embryonic patterning and cell fate determination (Chang et al., 2002). Activation of TGF-β signaling induces mesoderm- and endoderm-specific gene expression in a dose-dependent fashion in early *Xenopus* embryos. To examine whether RanBP3 can regulate TGF-β signaling during *Xenopus* embryogenesis, we examined the effects of RanBP3 on activin- or BMP-induced endogenous gene expression in *Xenopus* ectodermal explants (animal caps). As shown in Figure 1I, activin induced a whole range of mesendodermal markers, including the endodermal marker Sox17α, the dorsal mesodermal marker chordin, the ventrolateral mesodermal marker XWnt8, and the pan-mesodermal marker XBra at gastrula stages (lane 2), whereas BMP4 induced the expression of Sox17α, XWnt8 and Xbra (lane 5). Co-expression of wildtype RanBP3, but not RanBP3-wv, completely suppressed activin-induced expression of Sox17α and chordin, and moderately reduced the expression of Xbra and XWnt8 (lanes 3 and 4). In contrast, RanBP3 or RanBP3-wv failed to block the expression of the genes activated by BMP4, including Sox17α, Xwnt8 and XBra (lane 6). These results further support the notion that RanBP3 preferentially blocks activin but not BMP signaling in a Ran-binding dependent manner.

Knockdown of RanBP3 enhances TGF-β growth inhibitory and transcriptional responses

We next investigated whether RanBP3 depletion enhances TGF-β responses. We first established HaCaT cell lines that stably express distinct shRNAs against separate target sequences of RanBP3, i.e. shRNA494 (designated RanBP3-KD1) or shRNA-676 (designated RanBP3-KD2 and KD3)(Figure 2A and 2E). It is clear that depletion of RanBP3 enhanced TGF-β-induced expression of both the SBE-Luc reporter (Figure 2B) and the natural genes including those encoding PAI-1, and CDK inhibitors p15 and p21 (Figure 2C). Consistent with the increased mRNA levels of p15 and p21, depletion of RanBP3 rendered cells more sensitive to TGF-β-induced growth inhibition (Figure 2D and 2E). Collectively, these data established a novel role of RanBP3 as negative modulator in TGF-β-mediated transcriptional responses.

RanBP3 enhances nuclear export of Smad2/3

Because RanBP3 has been implicated in nuclear export by its ability to bind Ran, nuclear pore components and CRM1 (Mueller et al., 1998; Englmeier et al., 2001; Lindsay et al., 2001), we sought to evaluate if RanBP3 has a direct role in regulating Smad2/3 nuclear export. The ability of RanBP3 to affect TGF-β-induced nuclear accumulation of endogenous Smad3 was examined in HaCaT cells. As seen in Figure 3A, indirect immunostaining of Smad3 revealed

that overexpression of RanBP3 decreased the intensity of nuclear Smad3 by 55.3%(+/-4.2%). Similar results were observed with mouse RanBP3 (data not shown). To further confirm this observation, TGF-β-induced nuclear accumulation of endogenous Smad2 was examined in parental HaCaT cells, RanBP3-expressing stable cells (RanBP3-OE), and RanBP3 knockdown cells (RanBP3-KD1). The results demonstrate that the level of nuclear Smad2/3 is inversely proportional to that of RanBP3 in the nucleus. As shown in Figure 3B, TGF-β stimulation rapidly induced Smad2 accumulation in the nucleus in parent HaCaT cells. Increased expression of RanBP3 reduced the level of nuclear Smad2 in RanBP3-OE cells, whilst knockdown of endogenous RanBP3 expression rendered more endogenous Smad2 accumulated in the nucleus of RanBP3-KD1 cells.

To specifically evaluate Smad2/3 export without interference of continuous import, we next examined the TGF-β-induced nuclear accumulation of Smad2/3 in the presence of TβRI inhibitor SB431542, which blocks Smad2/3 phosphorylation in the cytoplasm and nuclear accumulation thereafter (Laping et al., 2002; Inman et al., 2002a). In parental HaCaT cells, Smad2 and Smad4 were accumulated in the nucleus after 2 h of TGF-β stimulation, but redistributed throughout the whole cells after removal of TGF-β and simultaneous addition of SB431542 for 2 h. Treatment with CRM1 inhibitor LMB blocked Smad4 but not Smad2 redistribution (Figure 3C, top panels). In RanBP3-KD1 cells, sustained Smad2 nuclear localization was observed in the absence or presence of LMB (Figure 3C, second row panels from the bottom). On the contrary, knockdown of RanBP3 did not affect the Smad4 cellular redistribution (Figure 3C, bottommost panels).

We next sought to specifically examine how much Smad2/3 are exported into the cytoplasm. To this end, cells were similarly treated as in Figure 3C and harvested at different time point during 4 h export process. Smad2/3 levels in the cytoplasmic vs. nuclear fractions at each time point were analyzed by Western blotting. The quality of cytoplasmic/nuclear fractionation was determined by the presence of cytoplasmic GADPH and nuclear Lamin A/C in the fractions. At time point 0 (immediately after 60 min TGF-β treatment), a very low level of Smad2/3 in the cytoplasmic fractions of both wildtype and knockdown cell lines was detected, indicating most of the Smad2/3 resided in the nucleus. SB431542 treatment promoted the cycling back of Smad2/3 in the cytoplasm in parental HaCaT cells, as indicated by the gradual increase in the level of cytoplasmic Smad2/3 and the corresponding decrease in the nuclear Smad2/3 (Figure 3D). In contrast, knockdown of RanBP3 slowed down the cytoplasmic-to-nuclear shift of Smad2/3 in RanBP3-KD1 cells (Figure 3D). Taken together, the data in Figure 3 support the notion that RanBP3 positively regulates the nuclear export of Smad2/3.

RanBP3 enhances Smad2 nuclear export in a Ran-binding dependent manner

Since RanBP3 is a Ran-binding protein, we sought to examine whether RanBP3 requires Ran to export Smad2/3 by using *in vitro* export assay. In these assays, HaCaT cells stably expressing GFP-Smad2 were first treated with TGF-β for 2 h to induce Smad2 nuclear accumulation, and then pulsed with digitonin for 5 min to permeabilize cell membrane. After washing, the remaining level of GFP-Smad2, which represented nuclear Smad2 that was not exported, was determined by Western blotting analysis. Several dosages of digitonin were tested to produce substantial loss of cytoplasmic proteins yet retain the intact nuclear envelope (Figure S1). To avoid over-permeabilization, we chose 30 ng/ml of digitonin in the subsequent assays. Proper cell membrane permeabilization was confirmed by lack of GAPDH in the total lysates of permeabilized cells (Figure 4A). In addition, functional integrity of the nuclear envelope was assessed by similar levels of GFP-Smad2 in digitonin-permeabilized and non-permeabilized cells at time point 0 (normalized against that of Lamin A/C) as well as the disappearance of cytoplasmic GADPH after 5 min of digitonin treatment (Figure 4A, lane 4). *In vitro* export of GFP-Smad2 was progressive over time, as indicated by a reduced level of GFP-Smad2 protein

(Figure 4A, lanes 4-6) or diminished GFP fluorescence (data not shown) in the permeabilized cells. Retention of GFP-Smad2 in the nucleus appeared to partially, if not completely, depend on Ran activity and energy because it decreased after addition of recombinant Ran proteins to the cells (lanes 9 and 10) and increased when incubated on ice (lanes 7 and 8).

We then analyzed the effect of the Ran-binding deficiency of RanBP3-wv on Smad2 export. Albeit at low efficiency, recombinant RanBP3 and RanBP3-wv proteins could similarly enter the nucleus of permeabilized cells (Figure S2). It is apparent that RanBP3 was capable of exporting Smad2 (Figure 4B, lanes 4 and 5). In sharp contrast, RanBP3-wv had no effect on Smad2 export *in vitro* (lanes 6 and 7). To further compare the effect of RanBP3 or RanBP3-wv mutant, we also used a highly sensitive quantitative export assay (Cullen, 2004), which has been previously used to analyze Smad2 nuclear export (Xu et al., 2002; Lin et al., 2006). Consistent with our data *in vitro*, we found that RanBP3 increased Smad2 export by 5.2-folds, whereas RanBP3-wv failed to produce any effects (Figure 4C). These results strongly suggest that RanBP3 promotes Smad2 nuclear export in a Ran-dependent manner.

RanBP3 specifically interacts with Smad2/3

Having established the role of RanBP3 in mediating nuclear export of Smad2/3, we investigated if RanBP3 could physically associate with Smads. Co-immunoprecipitation (co-IP) assay was used to examine the ability of RanBP3 to interact with Smads in transfected HEK293 cells. We detected the presence of RanBP3 in the immuno-complex of Smad2 (Figure 5A, lanes 2 and 3), but not in that of Smad1 (Figure 5A, lane 4-5). RanBP3 could also bind to Smad3 (Figure 5B, lanes 1 and 2), which is the closest homolog of Smad2 and also functions as TGF-β signal transducer. The interaction of RanBP3 with Smad4, a common Smad for both TGF-β and BMP signaling, was comparatively weaker (Figure 5B, lanes 3 and 4). Furthermore, immunoprecipitation of endogenous RanBP3 retrieved endogenous Smad2 and Smad3 proteins in human keratinocytes HaCaT (Figure 5C, lane 4). Taken together, these data reveal an interaction between RanBP3 and TGF-β-specific Smad2/3 under physiological conditions. Notably, activation of the TGF-β receptor appeared to decrease the Smad2/3-RanBP3 interaction (Figure 5C, lane 5, to be discussed later).

We further examined the RanBP3-Smad3 interaction by mapping their respective interacting domains. As shown in Figure 5D, both the N-terminal MH1 domain and C-terminal MH2 domain could bind to RanBP3 *in vitro*. The domains in RanBP3, namely the N-terminal domain (N), intermediate domain domain (F) and C-terminal Ran:GTP-binding domain (R) (Mueller et al., 1998; Lindsay et al., 2001), all associated with Smad3 yet weakly than the full-length RanBP3 (Figure 5E). Among all the domains, R apparently exhibited stronger affinity to Smad3 than N or F (Figure 5E, lane 4) and directly interacted with Smad3 *in vitro* (Figure 5F, lane 3).

To further identify the structural determinants that define the RanBP3-interacting specificity of Smad3, we generated a series of chimeras between Smad1 (unable to bind to RanBP3) and Smad3 (able to bind to RanBP3). In these chimeras, one or two domains of Smad3 were replaced with the counterpart(s) of Smad1 (Figure 5G, right panel). The ability of these chimeras to bind to RanBP3 was assessed and compared with wildtype Smad 3 in co-IP experiments. As observed earlier, RanBP3 interacted with wildtype Smad3, but not Smad1 (Figure 5G, lanes 2 and 3). RanBP3 also interacted with Smad1-Smad3 chimeras containing the MH1 and/or MH2 domain of Smad3 (Figure 5G, lanes 4, 5 and 7-9). However, RanBP3 did not interact with Smad131 with the linker region only of Smad3 (Figure 5G, lane 6), suggesting the MH1 and MH2 domain mediate the RanBP3-Smad3 interaction. Interestingly, among all the chimeras, Smad313, which contains both the MH1 and MH2 domains of Smad3, exhibited the strongest interaction with RanBP3 that is comparable to that of wildtype Smad3 (Figure 5G, lanes 3 and 8). Taken together, data in Figure 5 suggest that at least two different

epitopes in Smad3 are recognized by RanBP3 and cooperatively mediate the Smad3-RanBP3 interaction.

RanBP3 binds to Smad2/3 in their unphosphorylated forms

As shown in Figure 5, the interaction between RanBP3 and Smad2/3 was apparently weaker in the presence of active TGF-β signaling, either by expression of a constitutively active mutant form of TβRI, i.e. ALK5(T202D) (Figure 5A, lane 3) or TGF-β ligand stimulation (Figure 5C, lane 5). Since RanBP3 resides in the nucleus (Mueller et al., 1998) (Figures 3A and 3B), where Smad2/3 dephosphorylation by nuclear phosphatase PPM1A also occurs (Lin et al., 2006), we examined the effect of PPM1A on the RanBP3-Smad3 interaction. The level of TGF-β-induced Smad3 phosphorylation was reduced by PPM1A, but was not affected by overexpressed RanBP3 (Figure S4). Notably, increased expression of PPM1A clearly enhanced the association between RanBP3 and Smad3 (Figure 6A, lanes 3 and 4). These data support the notion that RanBP3 preferentially binds to dephosphorylated Smad2/3.

We then carried co-IP experiments to examine the Smad2 SXS motif mutant that either lacks the C-terminal serine phosphorylation (inactive, 2SA) or harbors phosphorylation-mimetic residues (active, 2SD). Analysis of the results revealed different binding affinity of these mutants toward RanBP3. As shown in Figure 6B, RanBP3 pulled down more Smad2(2SA) than Smad2(2SD) mutant (lanes 3 and 4). Since the SXS motif phosphorylation induces Smad2/3-Smad4 interaction, we sought to determine whether TGF-β-induced Smad2-Smad4 interaction contributed to the decreased association between Smad2 and RanBP3. As shown in Figure 6C, overexpression of Smad4 did not affect the interaction between RanBP3 and the Smad2(2SD) mutant (lanes 2 and 3), which readily interact with Smad4 in the absence of TGF-β stimulation (data not shown). Overexpression of RanBP3 also had no affect on the interaction between Smad2(2SD) mutant and Smad4 (Figure 6D). These data suggest that Smad4 and RanBP3 do not interfere with each other for binding to Smad2/3.

To further explore how the phosphorylation affects the RanBP3-Smad2/3 interaction, we carried out *in vitro* binding assays to examine the RanBP3 interaction with the recombinant Smad2 MH2 (aa 241–467) protein either in its phosphorylated or unphosphorylated form. The results revealed that GST-RanBP3 could bound to unphosphorylated Smad2 MH2 domain (Figure 6E, lane 1), but had no binding affinity to the phosphorylated Smad2 MH2 domain (Figure 6E, lane 2). Collectively, these data establish that RanBP3 preferentially binds to the unphosphorylated and recently dephosphorylated Smad2/3.

RanBP3 interacts with Smad2/3 in the nucleus

To identify the subcellular compartment where RanBP3 interacts with Smad2/3, we used a YFP-based fluorescence complementation system that allows easy visualization of protein interactions with microscopy (Hu et al., 2002). In this system, YFP fragment YN (aa 1-154) and YC (aa 155-238) were separately fused with each of the interacting protein partners. Protein interaction brings together the two YFP halves to reconstitute a functional YFP that produces a fluorescent signal. In HaCaT cells co-expressing YC-RanBP3 and YN-Smad3, YFP fluorescence was detected in the nucleus in the absence of TGF-β (Figure 6F, set a); similar results were observed when the reverse pair, i.e. YN-RanBP3 and YC-Smad2, were used (Figure 6F, set b). As negative controls, the YC-RanBP3/YN-vector pair and YN-Smad2/YC-vector pair did not yield fluorescence (Figure 6F, set c and d).

We next examined how the RanBP3-Smad2 interaction responds to TGF-β. As shown in Figure 6G, endogenous Smad2 resided in both the cytoplasm and the nucleus in HaCaT cell at the resting state (0.2% FBS treatment overnight). Whilst TGF-β stimulation for 2 h induced nuclear accumulation of Smad2, TβRI inhibitor SB431542 rendered Smad2 mostly accumulated in the

cytoplasm. The distribution of transiently expressed YC-Smad2 mimics endogenous Smad2. When YC-Smad2 and YN-RanBP3 were co-expressed, YFP fluorescence resided exclusively in the nucleus under all the conditions examined, strongly suggesting that RanBP3 interacts with Smad2/3 in the nucleus regardless TGF-β signaling.

RanBP3 does not affect the DNA-binding ability of Smad3

As RanBP3 also associates with the MH1 domain of Smad3 (Figure 5D, lane 2), we sought to examine whether RanBP3 would affect the Smad3's DNA-binding ability using DNA pulldown assay. The biotin-labeled SBE oligo comprises of four copies of the SBE sequences and was used to retrieve SBE-containing complex from the lysates of HaCaT control cells and RanBP3-KD1 stable cells. As shown in Figure 6H, TGF-β induced binding of Smad3 and Smad4 to biotinylated SBE (lane 3 and 5). RanBP3 was undetectable in the SBE-containing complex (lane 2 and 3), which is consistent with its position downstream of the Smad complex dissociation and dephosphorylation of Smad3. Moreover, RanBP3 depletion did not affect the level of SBE-bound Smad3 (lane 5), suggesting that RanBP3 would not affect the Smad3's DNA-binding activity.

RanBP3-R dominantly blocks Smad2 export and enhances TGF-β signaling

To evaluate how the RanBP3-Smad interaction modulates Smad2/3 export as well as TGF-β signaling, we explored the use of the Smad-interacting region in RanBP3 as a competitive inhibitor for this interaction. The RanBP3-R resides in the cytoplasm when exogenously expressed (Welch et al., 1999). Since RanBP3 interacts with Smad2/3 in the nucleus (Figure 6F and 6G) and partly through the R domain of RanBP3 (Figure 5E and 5F), we introduced the nuclear localization signal (NLS) in the N terminus of RanBP3-R (generating NLS-R) in order to force RanBP3-R to be localized in the nucleus. When NLS-R was co-transfected with RanBP3, the association of RanBP3 with Smad2 (Figure 7A) and Smad3 (Figure 7B) was disrupted in HEK293T cells, clearly demonstrating that RanBP3-R competes with RanBP3 for Smad2/3 binding. We then examined the effect of NLS-R in Smad2 export and TGF-β-induced transcriptional responses. Quantitative Smad2 export assay revealed NLS-R attenuated RanBP3-mediated Smad2 export in a dose-dependent manner (Figure 7C). Consistently, NLS-R enhanced the TGF-β-induced SBE-luc response in HaCaT cells (Figure 7D). Collectively, these data suggest that through its direct interaction with Smad2/3, RanBP3 mediates the nuclear export of Smad2/3 and hence function as a negative modulator in TGF-β signaling.

Discussion

Stringent control of activation and termination of TGF-β signaling is critical for normal cell physiology. Deregulation of the TGF-β signaling pathway has been associated with pathogenesis of cancer and other diseases (Massague et al., 2000; Bierie and Moses, 2006; ten Dijke and Arthur, 2007). Though much effort during the past decade has focused on activation of TGF-β signaling, increasing evidence suggests that modulation of TGF-β signaling decay also plays important roles in maintenance of a balanced signaling level. TGF-β signaling can be terminated by different ways, such as dephosphorylation of R-Smads, degradation of Smad proteins, or nuclear exclusion of Smad signal transducers. Recent work demonstrates that a phosphatase-dependent mechanism operates in the export of dephosphorylated Smad2 out of the nucleus during termination of TGF-β signaling (Inman et al., 2002b; Nicolas et al., 2004; Schmierer and Hill, 2005). Although PPM1A has been identified as a Smad2 phosphatase and can promote nuclear export of Smad2 (Lin et al., 2006), the exact export machinery that transports dephosphorylated Smad2 out of the nucleus has not been elucidated. In this study, we identify RanBP3 as the key component that mediates Smad2/3 nuclear export.

RanBP3 is a nuclear Ran-binding protein. In addition to its C-terminal domain that has the Ran-binding capacity, the N-terminal sequences of RanBP3 contain several FXFG motifs that are characteristic of a subgroup of nucleoporins (Mueller et al., 1998). The ability of RanBP3 to mediate nuclear export of Smad2/3 depends on its direct association with Smad2 and Smad3, as demonstrated by a series of biochemical and immunofluorescence experiments. RanBP3 interacts with Smad2/3 primarily with its C-terminal R domain, and it shows strong preference to unphosphorylated Smad2/3 (Figures 5 and 6). The binding occurs in the nucleus (Figures 6F and 6G), suggesting that dephosphorylation of activated Smad2/3 by phosphatases may be a prerequisite for RanBP3 binding and nuclear export. Indeed, the nuclear Smad phosphatase PPM1A facilitates, while receptor activation decreases, the RanBP3-Smad2/3 association (Figure 6A). As un- or de-phosphorylated Smad2 is most likely not in complex with Smad4, these findings support the notion that RanBP3-mediated Smad2/3 nuclear export is downstream of Smad dephosphorylation and/or the disassociation of Smad2/3 from Smad4. Thus, either unphosphorylated or recently dephosphorylated Smad2/3 serve as cargos for RanBP3-mediated nuclear export.

The function of RanBP3 in regulating Smad nuclear export is restricted to the TGF-β pathway. RanBP3 selectively inhibits activin/TGF-β, but not BMP, transcriptional responses in mammalian cells (Figure 1H) and *Xenopus* embryos (Figure 1I), in agreement with the cargo selection of RanBP3 (Figures 5A, 5B and 5G). This supports the notion that distinct mechanisms underlying R-Smad nuclear export operate in TGF-β and BMP pathways. It has been shown that both Smad1 and Smad4 utilize CRM1 to associate with NES in these Smads for their nuclear export (Xiao et al., 2001; Xiao et al., 2003). This process is thus susceptible to treatment with LMB, which impairs the function of CRM1. In contrast, nuclear export of Smad2/3 is resistant to LMB (Inman et al., 2002b; Nicolas et al., 2004; Schmierer and Hill, 2005). It is reported that Exportin 4, which is LMB-insensitive, interacts with Smad3 and promotes its nuclear export. It is of importance to note that the Exportin 4-binding regions locates in the Smad3 MH2 domain and is well conserved among all R-Smads (Kurisaki et al., 2006). It is thus possible that Exportin 4 may represent a general exporter for all Smads. In contrast, our data presented herein clearly suggest that RanBP3 selectively interacts with Smad2/3, through the cooperative binding to both the MH1 and MH2 domains, and specifically mediates the export of Smad2/3 out of the nucleus.

The functional consequence of RanBP3-dependent nuclear export of Smad2/3 is also assessed in our studies. The activity of RanBP3 controls the nuclear Smad2/3 level, which correlates well with the strength of the TGF-β signaling. Despite a few studies on Smad nuclear export, the physiological consequences of Smad nuclear export in TGF-β signaling have rarely been examined. It is reasonable to speculate that TGF-β signaling should be short-lived or impaired when Smad2/3 proteins are forced out of the nucleus. Indeed, overexpression of RanBP3 dampens Smad2/3-mediated transcriptional responses both in mammalian cells and in *Xenopus* embryos (Figures 1 and 2). Conversely, knockdown of RanBP3 expression causes retention of Smad2/3 in the nucleus and enhances TGF-β responses. Similar outcome can be achieved by disrupting the endogenous RanBP3-Smad2/3 interaction (Figure 7). Consistent with its inability to bind to Smad1 (and presumably Smad5 and Smad8), RanBP3 has no effects on the BMP-induced transcriptional responses in mammalian cells and in *Xenopus* embryos (Figures 1D and 1I). This further supports the notion that distinct mechanisms underlying R-Smad nuclear export operate in TGF-β and BMP pathways.

The observation that inhibition of RanBP3 enhances TGF-β signaling seems to contradict with a previous model, which implicates that continuous nucleocytoplasmic shuttling is required for continuous TGF-β signaling (Schmierer and Hill, 2005). The simplified model has not taken into account of the newly synthesized Smads (that can transmit signals into the nucleus) and the turnover of existing Smads. In the RanBP3 knockdown cells, there is significant

accumulation of dephosphorylated Smad2/3. Could the dephosphorylated Smad2/3 in the nuclear be partially active? Indeed, unphosphorylated Smad2 exhibits some transcriptional activity on *in vitro* chromatin templates (Ross et al., 2006). Alternatively, dephosphorylated Smad2/3 could be re-phosphorylated by unknown kinase(s) in the nucleus; however, this seems unlikely based on our observation that knockdown of RanBP3 did not dramatically increase the level of P-Smad2/3 in the nucleus (Figure 3D). Thus, the exact underlying mechanism for how accumulation dephosphorylated of Smad2/3 in the nucleus ultimately leads to increased TGF-β signaling remains to be further elucidated.

Our studies suggest that dephosphorylation of Smad2 and Smad3 by PPM1A (and/or other Smad phosphatases) precedes their nuclear export by RanBP3. However, a question arises on how RanBP3 facilitates nuclear export of Smad2/3. RanBP3 can partner with CRM1 in some cases, and it also binds weakly to nuclear pore components *in vitro* (Englmeier et al., 2001) as well as the small GTPase Ran (Mueller et al., 1998; Englmeier et al., 2001). Since inhibition of CRM1 by LMB does not promote nuclear accumulation of Smad2/3 (Xu et al., 2002; Kurisaki et al., 2006), the chance that CRM1 is involved in RanBP3-mediated export of Smad2/3 is rather slim. Ranbp3-R can disrupt the Ranbp3-Smad2/3 interaction, dominantly inhibit Smad2 export and enhance TGF-β transcriptional responses (Figures 7C and 7D), suggesting that the N-terminal region of RanBP3 is apparently needed for the export process. As the N-terminal sequences contain FXFG motifs that are homologous to those in certain nucleoporins, we favor the idea that RanBP3 may act directly as a nuclear exporter for Smad2/3 (Figure 7E). This notion is supported by recent discoveries that RanBP3 enhances nuclear export of β-catenin to terminate Wnt-signaling (Hendriksen et al., 2005) and is a negative regulator for STAT92E nuclear accumulation in *Drosophila* (Baeg et al., 2005). The similar dependence of Smad2/3 and β-catenin on RanBP3 for nuclear export suggests that RanBP3 may represent a new class of nuclear exporter, which regulates the localization of key signaling components to determine the duration and the strength of the signals in diverse signaling pathways.

Experimental Procedures

Expression plasmids and antibodies

Details on plasmids and antibodies used/made in the study are provided in the online supplemental materials.

Cell line and transfection

Human HaCaT, HEK293T and HepG2 cells were grown as described previously (Feng et al., 1998; Feng et al., 2000; Lin et al., 2006). HaCaT cells stably expressing EGFP-Smad2 were kindly provided by Caroline Hill (Nicolas et al., 2004). C2C12 cells were maintained as undifferentiated myoblasts in Dulbecco's modified Eagle's medium with high glucose supplemented with 10% fetal bovine serum. HaCaT cells were transfected with SuperFect (Qiagen), HEK293T cells and HepG2 cells with Lipofectin (Invitrogen) and C2C12 cells with LipofectAmine (Invitrogen).

Transcription reporter assays

Reporter plasmids SBE-Luc, p21-Luc (gift of Bert Vogelstein), p15-Luc (gift of Xiao-Fan Wang) and p800-Luc (gift of David Luskutoff) were used to measure TGF-β-induced transcription. Plasmid Id1-Luc (gift of Peter ten Dijke) was used to measure BMP-induced transcription. pSVβgal (Promega), which expresses β-galactosidase under the control of the SV40 early promoter, was co-transfected to allow normalization of transfection efficiency. The total amount of transfected DNA was adjusted to the same amount by addition of vector DNA when necessary. Reporter assays were carried out as described (Feng et al., 2000). Briefly, 20

to 24 h after transfection, cells were treated with TGF-β1 (2 ng/ul) or BMP2 (50 ng/ul) for 24 h. Cells were then harvested for measurement of luciferase and β-galactosidase activities. All assays were done in duplicates and all values were normalized for transfection efficiency against β-galactosidase activities.

RNA interference

The target sequences of shRNA-494 (nt 494-512 of coding region, AGAGCCCCAGAAAAATGAG) and shRNA-676 (nt 676-694, CCGCAACGAACTATTTCCT) (targeting both human RanBP3a and RanBP3b) were previously described (Hendriksen et al., 2005). Annealed sense and antisense DNA oligonucleotides were cloned into pSRG vector (Lin et al., 2006). Stable HaCaT cell lines expressing shRNA-494/676 or pSRG vector were generated and selected with 2 ug/ul of puromycin.

GST fusion protein, *in vitro* protein binding and pull-down assays

Glutathione S-transferase fusion proteins were prepared using a commercial kit (Amersham Pharmacia Biotech). *In vitro* translated (TNT kit, Promega) [^{35}S]-labeled protein was pre-cleared with 5 ug of GST protein for 1 h and then incubated with 5 ug of various GST-fusion proteins for 2 h in the binding buffer (50 mM Tris•HCl [pH7.5], 120 mM NaCl, 2 mM EDTA, 0.1% NP40). [^{35}S]-labeled proteins bound to GST-fusion proteins were retrieved on glutathione-Sepharose beads, separated by SDS-PAGE, and visualized by autoradiography. For comparing the binding of phosphorylated or unphosphorylated Smad2 to RanBP3, 500 ng of recombinant Smad2MH2 or phosphorylated Smad2MH2 (aa 241–467) (Lin et al., 2006) were incubated with GST-RanBP3. RanBP3-bound Smad2MH2 was examined via Western blot analysis.

Cell fractionation and *in vitro* export assay

HaCaT parental or its stable cells were treated with SB431542 with indicated time periods in the text and harvested with fractionation buffer (10 mM HEPES [pH7.9], 1.5 mM $MgCl_2$, 10 mM KCl, 0.5 mM DTT, 0.5% NP-40 and protease inhibitors) for 20 min on ice, and then fractionated by centrifugation. The fractions were analyzed on SDS-PAGE and subsequent Western blot analysis (Figure 3D).

HaCaT cells stably expressing GFP-Smad2 cells were first treated with TGF-β to induce nuclear accumulation of Smad2 (Figure 4A & 4B). Cells were permeabilized with digitonin on ice for 5 min, and then thoroughly washed 3 times with a cold transport buffer (20 mM HEPES [pH7.3], 110 mM potassium acetate, 5 mM sodium acetate, 2 mM DTT, 1 mM GTP, 1.0 mM EGTA and proteinase inhibitor). Cells were incubated for 60 min at 30°C in the transport buffer with addition of ATP regeneration system (Sigma; 1 mM ATP, 5 mM creatine phosphate, and 20 U/ml creatine phosphokinase) and RanBP3 or Ran. RanBP3 proteins were prepared from GST-RanBP3 by removing GST with Precission (Amersham), and Ran proteins were enriched by anti-Flag immunoprecipitation of cell lysates from HEK293T cells expressing Flag-Ran and eluted with Flag-peptide (Sigma). Cells were then rinsed 3 times with the cold transport buffer. Excess buffer was removed and permeabilized cells were resolved in SDS-loading buffer. The level of GFP-Smad2 was then analyzed by Western blot analysis.

Quantitative Smad2 export assay

A quantitative analysis of nuclear transport of Smad2 was previously described (Xu et al., 2002; Lin et al., 2006), using MS2 coat protein-fused Smad2 (gift of Joan Massagué) and pDM128/8xMS2 export reporter system (gift of Bryan Cullen) (Cullen, 2004). Briefly, HEK293T cells were transfected with plasmids for MS2-Smad2, CAT reporter

pDM128/8xMS2 and β-galactosidase plasmid (for normalization) and additional factors under examination. 45 h after transfection, cell lysates were analyzed for CAT activity using ELISA-based assay (Roche). Relative export activity is calculated by normalized the CAT activity with β-galactosidase activity in each samples.

DNA pulldown assay

DNA pulldown assay was essentially carried out as previously described (Feng et al., 2000; Feng et al., 2002). Briefly, HaCaT parental or its stable cells were treated with or without TGF-β for 2 h and collected in lysis buffer (10 mM HEPES pH 7.5, 150 mM NaCl, 1 mM $MgCl_2$, 0.5 mM EDTA, 0.5 mM DTT, and 0.1% NP-40, 10% glycerol). The cell lysates were incubated with 30 pmol biotinylated SBE oligonucleotides and 5 ug of poly(dI-dC) at 4°C for 16 hours. DNA-bound proteins were collected with streptavidin-beads (Dynabeads M-280 Invitrogen) for 2 h, washed extensively with the lysis buffer, and examined by Western blotting.

Immunoprecipitation and Western blot analysis

Endogenous or epitope-tagged proteins were immunoprecipitated from cell lysates by appropriate antibody affinity gel as indicated in the text and figure legends. After extensive washes, immunoprecipitated proteins were eluted in SDS sample loading buffer (Bio-Rad), separated by SDS-PAGE, transferred to nitrocellulose (Pierce), and detected in Western blots with appropriate primary antibodies coupled with horseradish peroxidase-conjugated secondary antibody by chemiluminescence (Pierce).

Cell proliferation assays

Cells were grown in 96-well plates (3,000 cells per well) in cell culture medium supplemented with 0.2% fetal bovine serum (FBS) for overnight before TGF-β treatment. Cell proliferation was measured in duplicates for 3 days. Each harvest was incubated with 20 ul of CellTiter 96 AQueous One Solution Reagent (Promega) for 3 h at 37°C in the 5% CO_2 incubator. The absorbance at 490nm was obtained using the VersaMax microplate reader (Molecular Devices).

Xenopus gene expression analysis

RNAs used for microinjection into *Xenopus* embryos were synthesized with SP6 RNA polymerase using mMessage mMachine kit (Ambion). DNA templates were: AscI-linearized pCS105-RanBP3, pCS105-RanBP3-wv, EcoRI-linearized pSP64T-activin, and AscI-linearized pCS105-BMP4. RNAs were injected alone or in combination into the animal poles of two-cell stage embryos. The doses of RNAs used were RanBP3 or RanBP3-wv (1 ng), activin (1 pg), and BMP4 (20 pg). Ectodermal explants (animal caps) from injected embryos were obtained at blastula stages (stage 9) and incubated to gastrula stages (stage 11), at which time total RNA was extracted from these caps, and the gene expression pattern was analyzed by reverse transcription (RT)-PCR. The primers used in RT-PCR were as described (Chang et al., 1997).

Real-Time RT-PCR (qRT-PCR)

qRT-PCR was carried out using Assay-on-Demand kits (Applied Biosystem) and previously described (Lin et al., 2006). Briefly, total RNAs were prepared using TriZol reagent (Invitrogen) from HaCaT cells. mRNA levels of target genes p15, p21 and PAI-1 were normalized against 18S RNA. Each target was measured in triplicates.

Bimolecular fluorescence complementation (BiFC)

To set up a BiFC system (Hu et al., 2002), we created two expression plasmids pXF1YN and pXF1YC that contain aa 1-154 of enhanced YFP (designated YN) or 155-238 (designated YC), respectively. YN or YC-tagged Smads or RanBP3b were constructed by inserting the corresponding coding sequences into EcoRI and SalI sites of pXF1YN or pXF1YC. These expression plasmids were transfected into HaCaT cells, and 48 h after transfection, the fluorescence production was detected with a Zeiss Axiovert 200M microscope.

Immunofluorescence

Cells grown on coverslips were fixed with 4% formaldehyde for 30 min at 4°C, followed by 0.5% Triton X-100 treatment for 30 min and blocked with 5% milk in PEM buffer (400 mM Potassium PIPES [pH 6.8], 0.8 mM EGTA, 5 mM $MgCl_2$). Cells were then probed with primary antibodies, followed by Alexa Fluor 546 or Alexa Fluor 594 secondary antibody (Molecular Probes). Fluorescence images were acquired with a Zeiss Axiovert 200M microscope.

Supplementary Material

Refer to Web version on PubMed Central for supplementary material.

Acknowledgments

We thank Bryan Cullen, Maarten Fornerod, Caroline S. Hill, Mien-Chie Hung, Tom Kerppola, Ed Leof, Joan Massagué, Yigong Shi, Peter ten Dijke, and Bert Vogelstein for numerous reagents that make this study possible. Thanks also go to Hongyan Xu for helpful discussion with statistics analysis, Feng Liu for technical assistance, and members of Feng and Lin labs for continuous stimulating discussion. This research was supported by NIH grants (R01AR053591 and R01CA108454 to X.-H.F., R01DK073932 to X.L., R01HD43345 to C.C.). X.-H.F is a Leukemia and Lymphoma Society Scholar.

Reference List

Baeg GH, Zhou R, Perrimon N. Genome-wide RNAi analysis of JAK/STAT signaling components in Drosophila. Genes and Development 2005;19:1861–1870. [PubMed: 16055650]

Bierie B, Moses HL. TGF beta: the molecular Jekyll and Hyde of cancer. Nature Reviews Cancer 2006;6:506–520.

Chang C, Wilson PA, Mathews LS, Hemmati-Brivanlou A. A Xenopus type I activin receptor mediates mesodermal but not neural specification during embryogenesis. Development 1997;124:827–837. [PubMed: 9043064]

Chang H, Brown CW, Matzuk MM. Genetic analysis of the mammalian transforming growth factor-beta superfamily. Endocr Rev 2002;23:787–823. [PubMed: 12466190]

Cullen BR. Assaying nuclear messenger RNA export in human cells. Methods Mol Biol 2004;257:85–92. [PubMed: 14769998]

Derynck, R.; Miyazono, K. The TGF-beta Family. Cold Spring Harbor Laboratory Press; 2007.

Englmeier L, Fornerod M, Bischoff FR, Petosa C, Mattaj IW, Kutay U. RanBP3 influences interactions between CRM1 and its nuclear protein export substrates. EMBO Rep 2001;2:926–932. [PubMed: 11571268]

Feng XH, Derynck R. Specificity and versatility in TGF-beta signaling through Smads. Annual Review of Cell and Developmental Biology 2005;21:659–693.

Feng XH, Liang YY, Liang M, Zhai W, Lin X. Direct interaction of c-Myc with Smad2 and Smad3 to inhibit TGF-beta-mediated induction of the CDK inhibitor p15(Ink4B). Mol Cell 2002;9:133–143. [PubMed: 11804592]

Feng XH, Lin X, Derynck R. Smad2, Smad3 and Smad4 cooperate with Sp1 to induce p15(Ink4B) transcription in response to TGF-beta. EMBO J 2000;19:5178–5193. [PubMed: 11013220]

Feng XH, Zhang Y, Wu RY, Derynck R. The tumor suppressor Smad4/DPC4 and transcriptional adaptor CBP/p300 are coactivators for smad3 in TGF-beta-induced transcriptional activation. Genes Dev 1998;12:2153–2163. [PubMed: 9679060]

Hendriksen J, Fagotto F, van d V, van SM, Noordermeer J, Fornerod M. RanBP3 enhances nuclear export of active (beta)-catenin independently of CRM1. J Cell Biol 2005;171:785–797. [PubMed: 16314428]

Hu CD, Chinenov Y, Kerppola TK. Visualization of interactions among bZip and Rel family proteins in living cells using bimolecular fluorescence complementation. Molecular Cell 2002;9:789–798. [PubMed: 11983170]

Inman GJ, Nicolas FJ, Callahan JF, Harling JD, Gaster LM, Reith AD, Laping NJ, Hill CS. SB-431542 is a potent and specific inhibitor of transforming growth factor-beta superfamily type I activin receptor-like kinase (ALK) receptors ALK4, ALK5, and ALK7. Molecular Pharmacology 2002a; 62:65–74. [PubMed: 12065756]

Inman GJ, Nicolas FJ, Hill CS. Nucleocytoplasmic shuttling of Smads 2, 3, and 4 permits sensing of TGF-beta receptor activity. Mol Cell 2002b;10:283–294. [PubMed: 12191474]

Kurisaki A, Kose S, Yoneda Y, Heldin CH, Moustakas A. Transforming growth factor-beta induces nuclear import of Smad3 in an importin-beta 1 and Ran-dependent manner. Molecular Biology of the Cell 2001;12:1079–1091. [PubMed: 11294908]

Kurisaki A, Kurisaki K, Kowanetz M, Sugino H, Yoneda Y, Heldin CH, Moustakas A. The mechanism of nuclear export of Smad3 involves exportin 4 and Ran. Mol Cell Biol 2006;26:1318–1332. [PubMed: 16449645]

Laping NJ, Grygielko E, Mathur A, Butter S, Bomberger J, Tweed C, Martin W, Fornwald J, Lehr R, Harling J, Gaster L, Callahan JF, Olson BA. Inhibition of transforming growth factor (TGF)-beta 1-induced extracellular matrix with a novel inhibitor of the TGF-beta type I receptor kinase activity: SB-431542. Molecular Pharmacology 2002;62:58–64. [PubMed: 12065755]

Lin X, Duan XY, Liang YY, Su Y, Wrighton KH, Long JY, Hu M, Davis CM, Wang JR, Brunicardi FC, Shi YG, Chen YG, Meng AM, Feng XH. PPM1A functions as a Smad phosphatase to terminate TGF beta signaling. Cell 2006;125:915–928. [PubMed: 16751101]

Lindsay ME, Holaska JM, Welch K, Paschal BM, Macara IG. Ran-binding protein 3 is a cofactor for Crm1-mediated nuclear protein export. J Cell Biol 2001;153:1391–1402. [PubMed: 11425870]

Massague J, Blain SW, Lo RS. TGF beta signaling in growth control, cancer, and heritable disorders. Cell 2000;103:295–309. [PubMed: 11057902]

Massague J, Seoane J, Wotton D. Smad transcription factors. Genes and Development 2005;19:2783–2810. [PubMed: 16322555]

Mueller L, Cordes VC, Bischoff FR, Ponstingl H. Human RanBP3, a group of nuclear RanGTP binding proteins. FEBS Lett 1998;427:330–336. [PubMed: 9637251]

Nicolas FJ, De BK, Schmierer B, Hill CS. Analysis of Smad nucleocytoplasmic shuttling in living cells. J Cell Sci 2004;117:4113–4125. [PubMed: 15280432]

Pierreux CE, Nicolas FJ, Hill CS. Transforming growth factor beta-independent shuttling of Smad4 between the cytoplasm and nucleus. Mol Cell Biol 2000;20:9041–9054. [PubMed: 11074002]

Ross S, Cheung E, Petrakis TG, Howell M, Kraus WL, Hill CS. Smads orchestrate specific histone modifications and chromatin remodeling to activate transcription. EMBO J 2006;25:4490–4502. [PubMed: 16990801]

Schmierer B, Hill CS. Kinetic analysis of Smad nucleocytoplasmic shuttling reveals a mechanism for transforming growth factor beta-dependent nuclear accumulation of Smads. Mol Cell Biol 2005;25:9845–9858. [PubMed: 16260601]

ten Dijke P, Arthur HM. Extracellular control of TGF beta signalling in vascular development and disease. Nature Reviews Molecular Cell Biology 2007;8:857–869.

ten Dijke P, Hill CS. New insights into TGF-beta-Smad signalling. Trends in Biochemical Sciences 2004;29:265–273. [PubMed: 15130563]

Watanabe M, Masuyama N, Fukuda M, Nishida E. Regulation of intracellular dynamics of Smad4 by its leucine-rich nuclear export signal. EMBO Rep 2000;1:176–182. [PubMed: 11265759]

Welch K, Franke J, Kohler M, Macara IG. RanBP3 contains an unusual nuclear localization signal that is imported preferentially by importin-alpha3. Mol Cell Biol 1999;19:8400–8411. [PubMed: 10567565]

Xiao Z, Brownawell AM, Macara IG, Lodish HF. A novel nuclear export signal in Smad1 is essential for its signaling activity. J Biol Chem 2003;278:34245–34252. [PubMed: 12821673]

Xiao Z, Liu XD, Lodish HF. Importin beta mediates nuclear translocation of Smad 3. Journal of Biological Chemistry 2000;275:23425–23428. [PubMed: 10846168]

Xiao Z, Watson N, Rodriguez C, Lodish HF. Nucleocytoplasmic shuttling of Smad1 conferred by its nuclear localization and nuclear export signals. J Biol Chem 2001;276:39404–39410. [PubMed: 11509558]

Xu L, Alarcon C, Col S, Massague J. Distinct domain utilization by Smad3 and Smad4 for nucleoporin interaction and nuclear import. J Biol Chem 2003;278:42569–42577. [PubMed: 12917407]

Xu L, Chen YG, Massague J. The nuclear import function of Smad2 is masked by SARA and unmasked by TGF beta-dependent phosphorylation. Nature Cell Biology 2000;2:559–562.

Xu L, Kang Y, Col S, Massague J. Smad2 nucleocytoplasmic shuttling by nucleoporins CAN/Nup214 and Nup153 feeds TGFbeta signaling complexes in the cytoplasm and nucleus. Mol Cell 2002;10:271–282. [PubMed: 12191473]

Zawel L, Dai JL, Buckhaults P, Zhou S, Kinzler KW, Vogelstein B, Kern SE. Human Smad3 and Smad4 are sequence-specific transcription activators. Mol Cell 1998;1:611–617. [PubMed: 9660945]

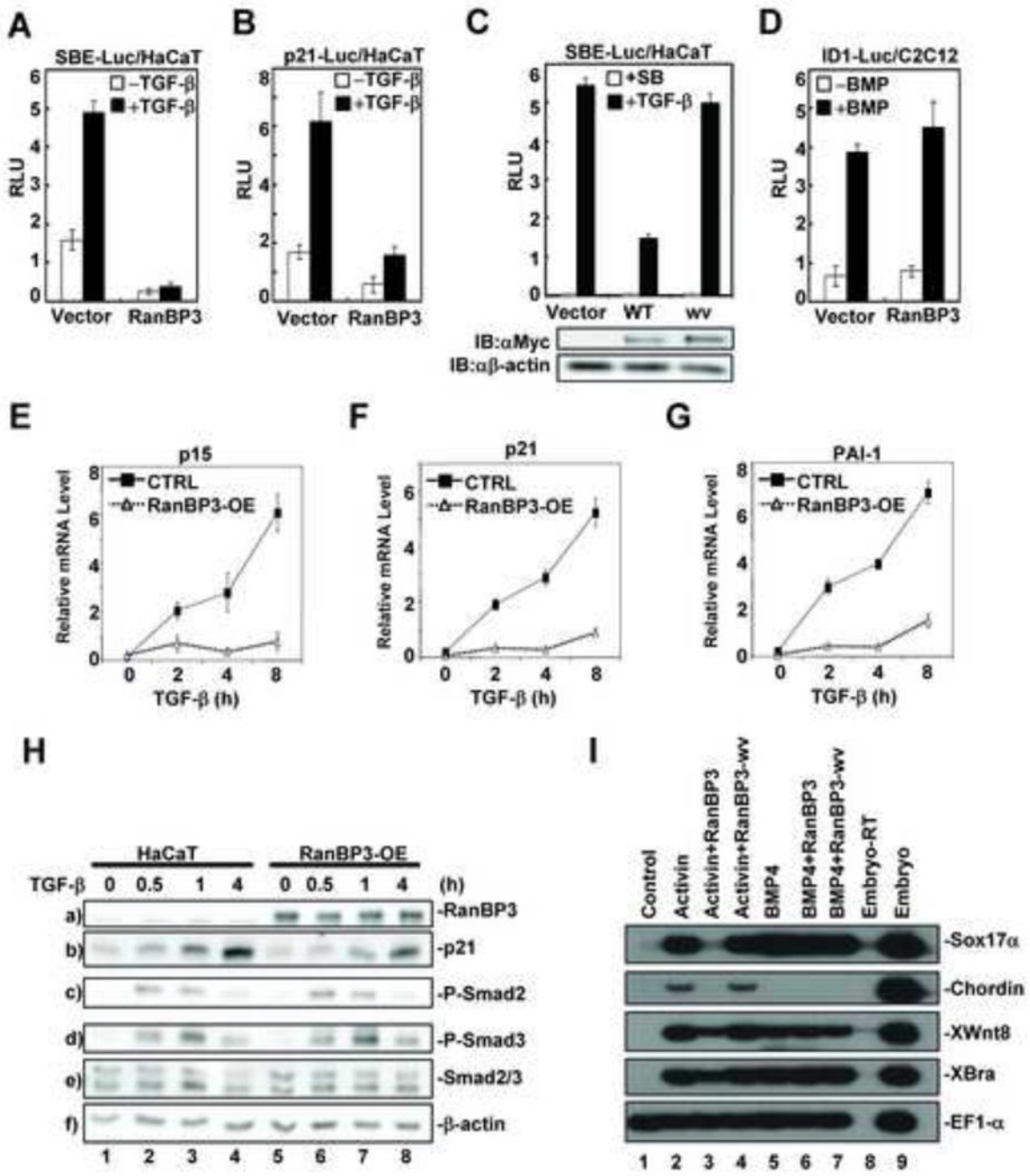

Figure 1. RanBP3 inhibits TGF-β-induced transcriptional responses in mammalian cells

(A) The SBE-luc reporter activity was measured in HaCaT cells that were co-transfected with Myc-RanBP3 and treated with 2 ng/ml of TGF-β (20 h). Values and error bars represent mean and standard deviation of three experiments.

(B) Effect of RanBP3 on the natural p21 promoter in HaCaT cells.

(C) RanBP3-wv, defective in Ran-binding, fails to affect SBE-luc response. SBE-Luc reporter was co-transfected into HaCaT cells with Myc-RanBP3 (WT) or Myc-RanBP3-wv (wv), and treated with SB431542 (SB) or TGF-β. The expression level of RanBP3 (TGF-β-treated) was examined by using Western blotting (bottom).

(D) Effect of RanBP3 on BMP responses. C2C12 cells were transfected with Myc-RanBP3 and Id1-Luc reporter. Luciferase activity was measured 20 h after treatment with 25 ng/ml of BMP2.
(E) Quantitative real-time RT-PCR (qRT-PCR) analysis of *p15* mRNA. RanBP3-OE (stably expressing Flag-RanBP3) cells and parental HaCaT cells were stimulated with TGF-β up to 8 h before total RNAs were harvested.
(F) qRT-PCR analysis of *p21* mRNA.
(G) qRT-PCR analysis of *PAI-1* mRNA.
(H) Western analysis of p21 protein. RanBP3-OE or parental HaCaT cells were treated with TGF-β for 4 h and harvested at indicated times. The expression levels of RanBP3, p21, Smad2/3 and Smad2/3 phosphorylation were examined by Western blotting with appropriate antibodies as indicated. β-actin blot serves as a loading control.
(I) Mesodermal and endodermal marker induction in *Xenopus* ectodermal explants. The gene expression in uninjected control animal caps (lane 1), and in whole embryos processed in the absence or presence of reverse transcriptase in RT-PCRs (lanes 8 and 9) are shown. The expression level of EF-1α is used as the loading control.

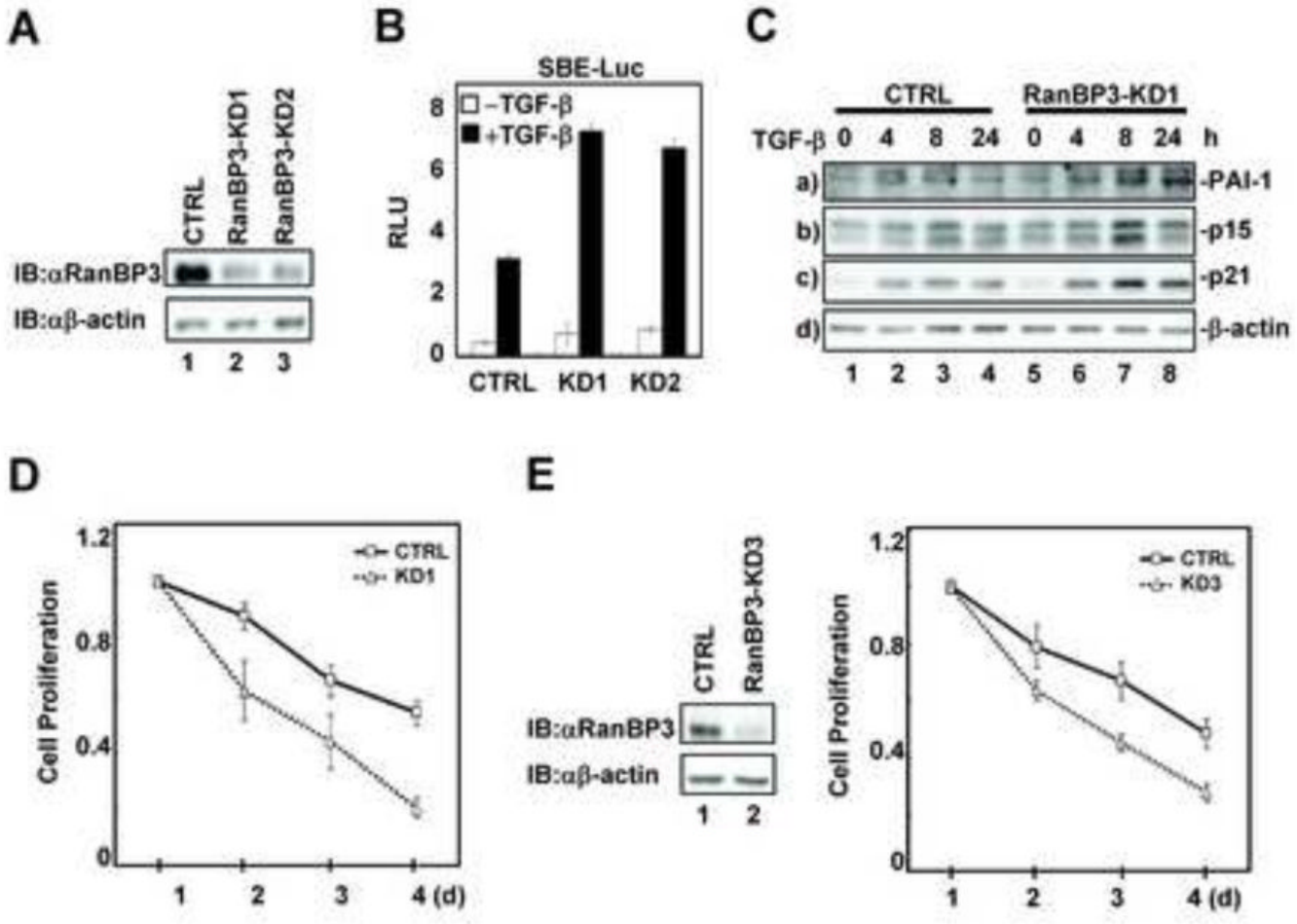

Figure 2. Knockdown of RanBP3 enhances TGF-β growth inhibitory and transcriptional responses

(A) RanBP3 expression in HaCaT cell lines stably expressing RanBP3 shRNAs was examined by anti-RanBP3 western blotting. Whole cell lysates were prepared from HaCaT cell lines stably expressing shRNA-494 (designated RanBP3-KD1), shRNA-676 (RanBP3-KD2) or empty pSRG vector (CTRL). β-actin serves as a loading control.

(B) Luciferase activity of SBE-Luc was examined in RanBP3 knockdown stable cells and control HaCaT cells.

(C) Western blotting analysis of PAI-1, p15 and p21. Whole cell lysates from RanBP3-KD1 and control HaCaT cells were immunoblotted with antibodies shown on the right. An anti-β-actin immunoblot serves as a loading control.

(D) Proliferation of HaCaT stable clone RanBP3-KD1 and control cells was examined using MTT assays (Promega) according to manufacture's instructions.

(E) Proliferation of HaCaT stable clone RanBP3-KD3 and control cells. RanBP3 expression was examined by anti-RanBP3 western blotting (left).

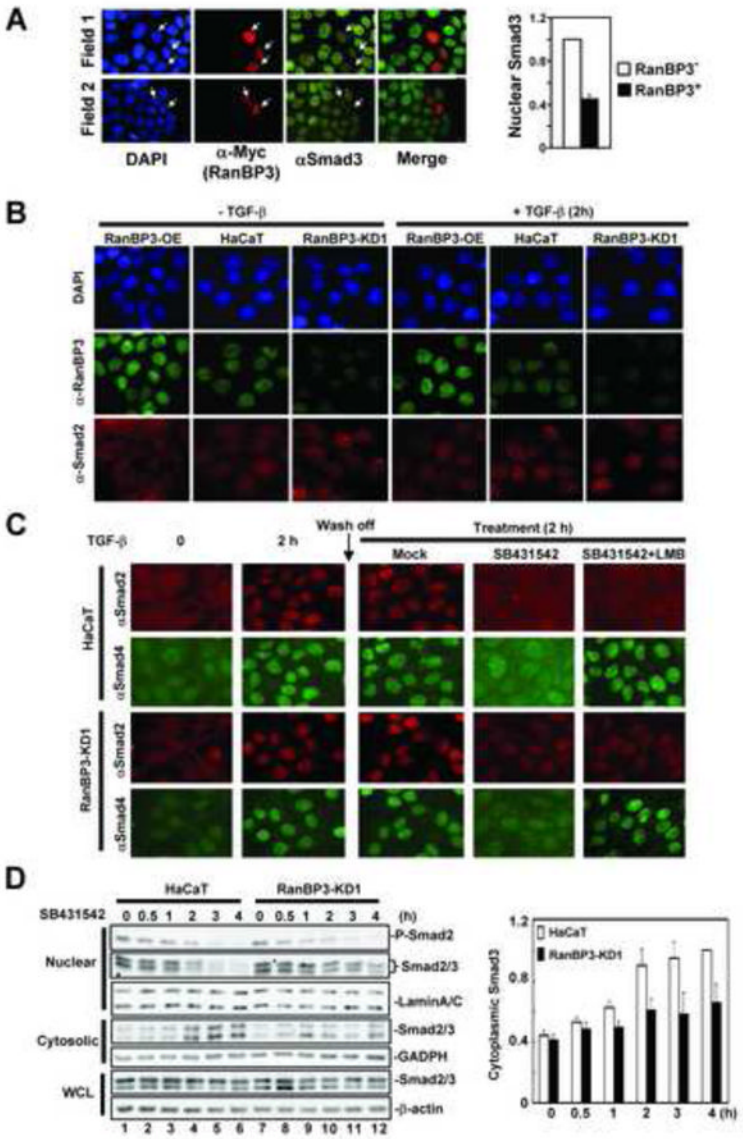

Figure 3. RanBP3 enhances nuclear export of Smad2/3

(A) Smad3 nuclear accumulation. HaCaT cells were transfected with Myc-RanBP3, and 24 h after transfection, treated with TGF-β for 2 h and fixed. The localization of endogenous Smad3 was examined by indirect immunostaining with anti-Smad3 antibody. Cells that received Myc-RanBP3 were demonstrated by anti-Myc immunostaining, indicated by white arrows. Quantification of nuclear Smad3 (immunostaining intensity) in RanBP3-transfected cells ($RanBP3^+$, n=15) and RanBP3 non-transfected cells ($RanBP3^-$, n=45) from multiple experiments were shown on the right. Error bars represent standard deviation.

(B) Distribution of Smad2. HaCaT stable cells expressing Flag-RanBP3 (RanBP3-OE) or shRanBP3-433 (RanBP3-KD1) as well as parental cells were treated with TGF-β for 2 h and fixed. RanBP3 and Smad2 were visualized by indirect immunostaining with anti-RanBP3 or anti-Smad2 antibodies, respectively.

(C) Effect of RanBP3 depletion on the level of nuclear Smad2. RanBP3-KD1 and parental HaCaT cells were treated with TGF-β for 2 h to induce nuclear accumulation of Smad2. Cells were washed 3 times to remove TGF-β and then treated with SB431542 (5 nM) and/or LMB (20 ng/ml) for another 2 h before fixation. Endogenous Smad2 and Smad4 were visualized by

indirect immunostaining with anti-Smad2 and anti-Smad4 antibodies, respectively. Fluorescence images were acquired with the same exposure parameters for intensity comparison.

(D) Cytoplasmic and nuclear fractionation. RanBP3-KD1 and parental HaCaT cells were treated with TGF-β for 1 h, cells were washed 3 times to remove TGF-β and treated with SB431542 up to 4 h. After cells were then harvested at indicated time, both the nuclear and cytoplasmic fractions were collected. The total Smad2/3 levels as well as the P-Smad2 level were examined. The nuclear-localized protein Lamin A/C and cytoplasmic-localized protein GADPH demonstrate separation of the fractions and proper sample loading. Relative level of cytoplasmic Smad3 (Smad3/GAPDH) was quantified using NIH image. The arbitrary unit for cytoplasmic Smad3 in control cells at 4 h of SB431542 treatment was set to 1. Values and error bars represent mean and standard deviation of three experiments.

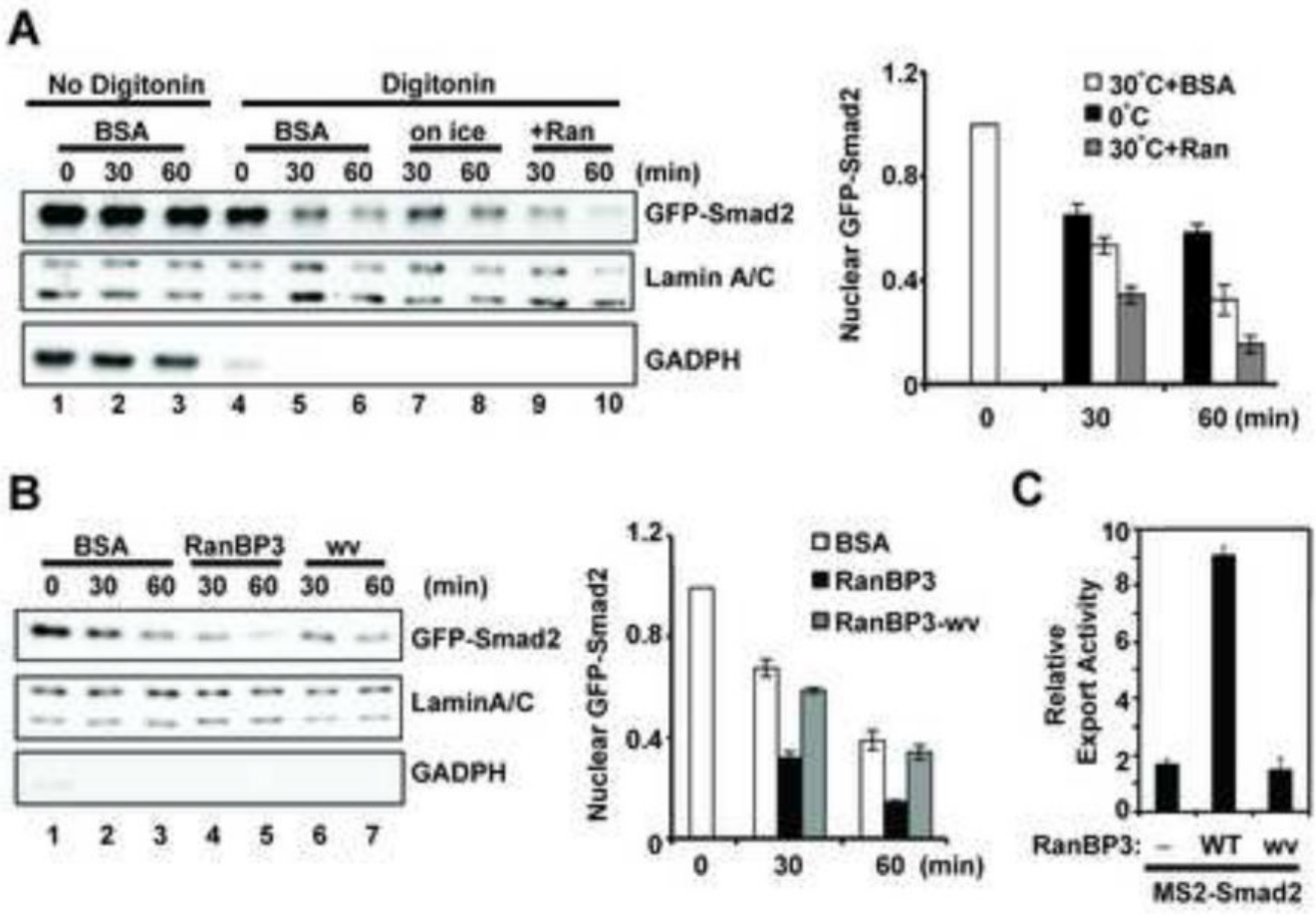

Figure 4. RanBP3 mediates Smad2 export dependent of its Ran-binding ability

(A) *In vitro* export of Smad2. Stable HaCaT cells expressing GFP-Smad2 were permeabilized with digitonin (30 ng/ml) for 5 min and then incubated in a reaction buffer containing either BSA or Ran at 30°C or on ice. GFP-Smad2 was examined by anti-Smad2 antibody Western blotting (~80 kDa). Lamin A/C and GADPH indicate levels of nuclear and cytoplasmic proteins. Relative level of nuclear GFP-Smad2 (Smad2:Lamin A) was quantified from multiple experiments. The arbitrary unit for nuclear GFP-Smad2 in lane 4 was set to 1. Values and error bars represent mean and standard deviation of three experiments.

(B) The effect of RanBP3 or RanBP3-wv protein on Smad2 export.

(C) A quantitative Smad2 export assay (see Experimental Procedures) was used to examine the effect of RanBP3 or RanBP3-wv mutant on Smad2 export. Values and error bars represent mean and standard deviation of three experiments.

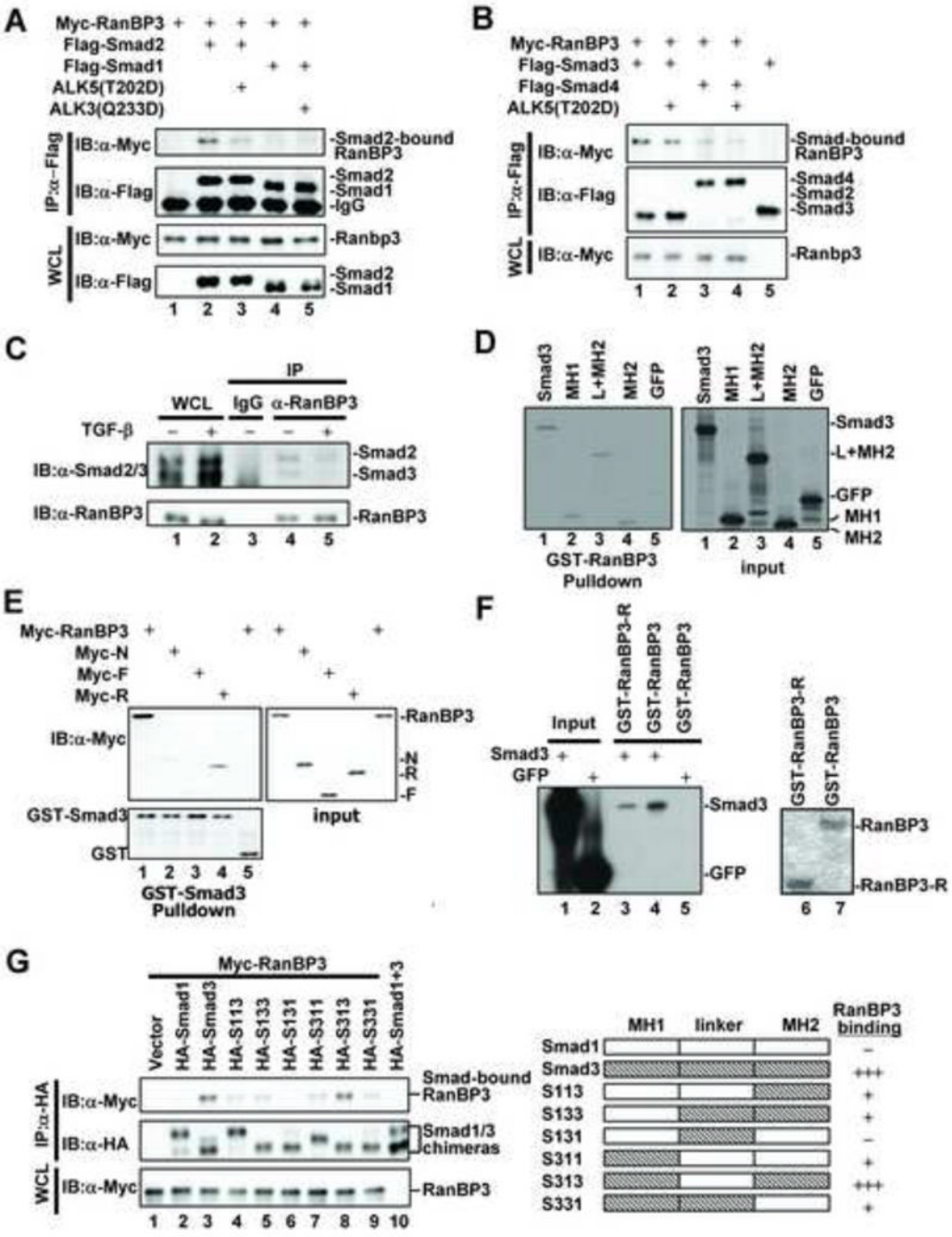

Figure 5. RanBP3 interacts with TGF-β specific Smad2 and Smad3

(A) Co-immunoprecipitation (Co-IP) of Smads and RanBP3. HEK293T cells were transfected with indicated expression plasmids for RanBP3, Smad1 or 2, and a constitutively active receptor ALK5(T202D) (lane 3) or ALK3(Q233D) (lane 5). Levels of Smads and RanBP3 in the IP products and whole cell lysates (WCL) were analyzed by Western blotting.

(B) Co-IP of RanBP3 and Smad3.

(C) Endogenous RanBP3-Smad2/3 interaction. HaCaT cells at 90% confluency were treated with or without TGF-β for 2 h before harvest. RanBP3-bound Smad2/3 were immunoprecipitated with an anti-RanBP3 antibody and detected by anti-Smad2/3 Western blotting. The anti-mouse IgG immunoprecipitates in lane 3 serve as negative control.

(D) Mapping of RanBP3-binding domains of Smad3. [S^{35}]-labeled Smad3 MH1 domain, MH2 domain as well as the linker region plus MH2 domain was incubated with GST-RanBP3 protein on glutathione beads. Retrieved proteins were separated by SDS-PAGE and visualized by autoradiography. GFP serves as a negative control.
(E) Mapping of Smad-binding domains of RanBP3.
(F) Ran-binding domain of RanBP3 (RanBP3-R) interacts with Smad3 in GST-pulldown assay.
(G) The MH1 and MH2 domains confer the maximum binding of Smad3 to RanBP3. HEK293T cells were transfected with Myc-RanBP3, Flag-Smad1, Flag-Smad3 as well as Flag-Smad1/3 domain chimera as indicated. Co-IP experiments were conducted similarly as in A.

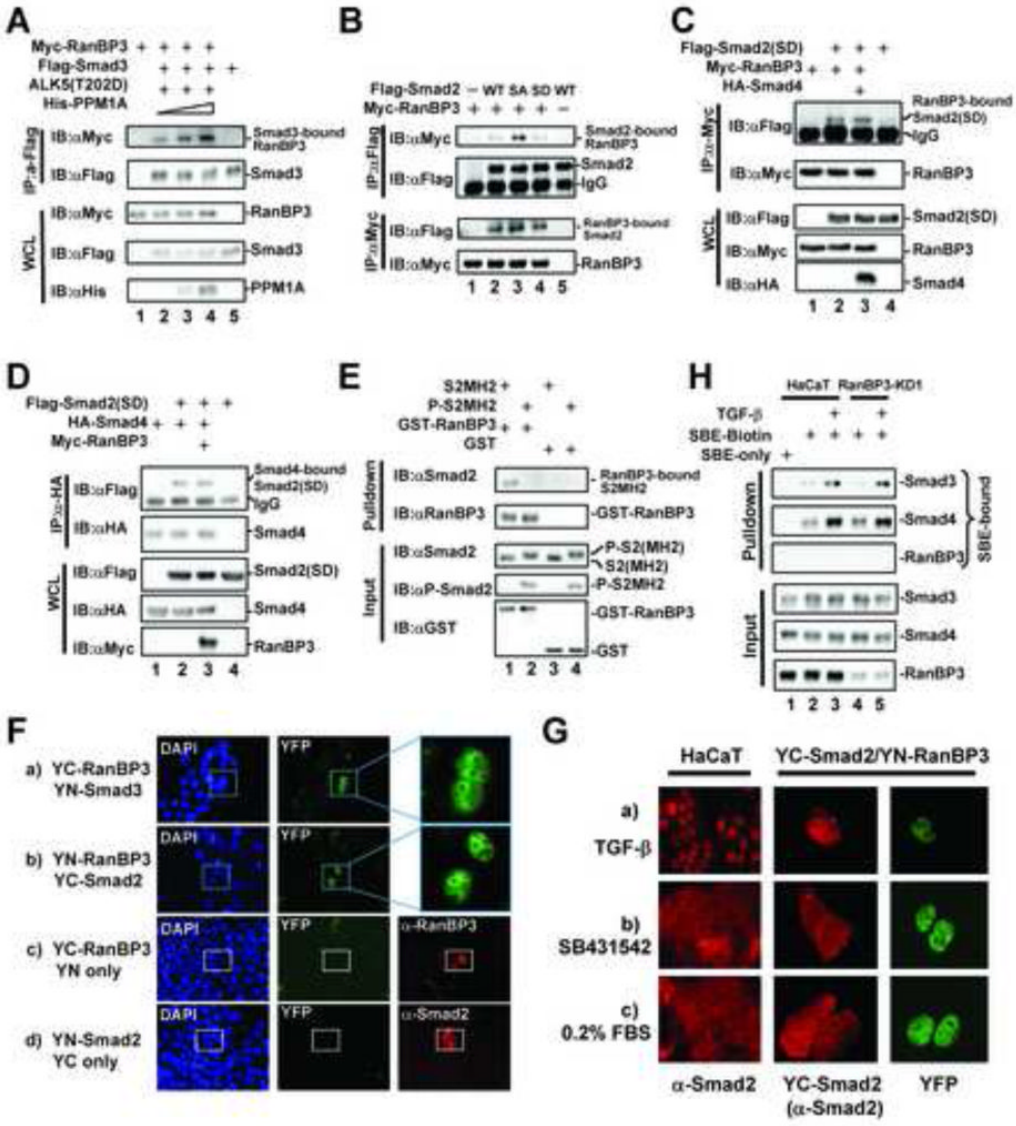

Figure 6. RanBP3 binds to Smads in its unphosphorylated form in the nucleus

(A) Effect of increasing dosages of PPM1A on the Smad3-RanBP3 interaction. HEK293T cells were transfected with expression plasmids as indicated.

(B) Binding of RanBP3 to Smad3 mutants in co-IP experiments. Myc-RanBP3 was co-transfected into HEK293T cells with Smad2 wild type (WT), Smad2 mutant lacking the C-terminal serine phosphorylation (2SA), or active Smad2 mutant harboring C-terminal serine phosphorylation-mimetic residues (2SD).

(C) The interaction between Myc-RanBP3 and Flag-Smad2(2SD) in the presence of HA-Smad4.

(D) Effect of RanBP3 on the interaction between HA-Smad4 and Flag-Smad2(2SD).

(E) Binding of RanBP3 to the un-phosphorylated MH2 domain of Smad2 (S2MH2). Recombinant S2MH2 or phosphorylated S2MH2 (P-S2MH2) was incubated with GST-RanBP3 proteins (or GST only as negative control) on glutathione beads. S2MH2 or GST proteins were demonstrated by Western blots with anti-Smad2 or anti-GST antibody, respectively.

(F) Visualization of the RanBP3-Smad2/3 interactions in BiFC assays. HaCaT cells were co-transfected with expression plasmids as indicated. Images of reconstituted YFP fluorescence (cells in cyan boxes) were acquired 24 h after transfection. Cells that received the YC-RanBP3/YN pair or the YN-Smad2/YC pair were also immunostained with anti-RanBP3 (image c) or anti-Smad2 antibody (image d), respectively. DAPI staining indicates the nucleus.
(G) Effect of TGF-β on the RanBP3-Smad3 interaction in BiFC assays. YC-RanBP3/YN-Smad3 co-transfected HaCaT cells were treated for 2 h with TGF-β (a), overnight with SB431542 (b) or 0.2% FBS (c).
(H) DNA-binding assay of Smad3. The DNA-Smad complex was affinity-purified using biotinylated SBE from RanBP3-KD1 cells and parent HaCaT cells, and then examined by using Western blotting with the indicated antibodies.

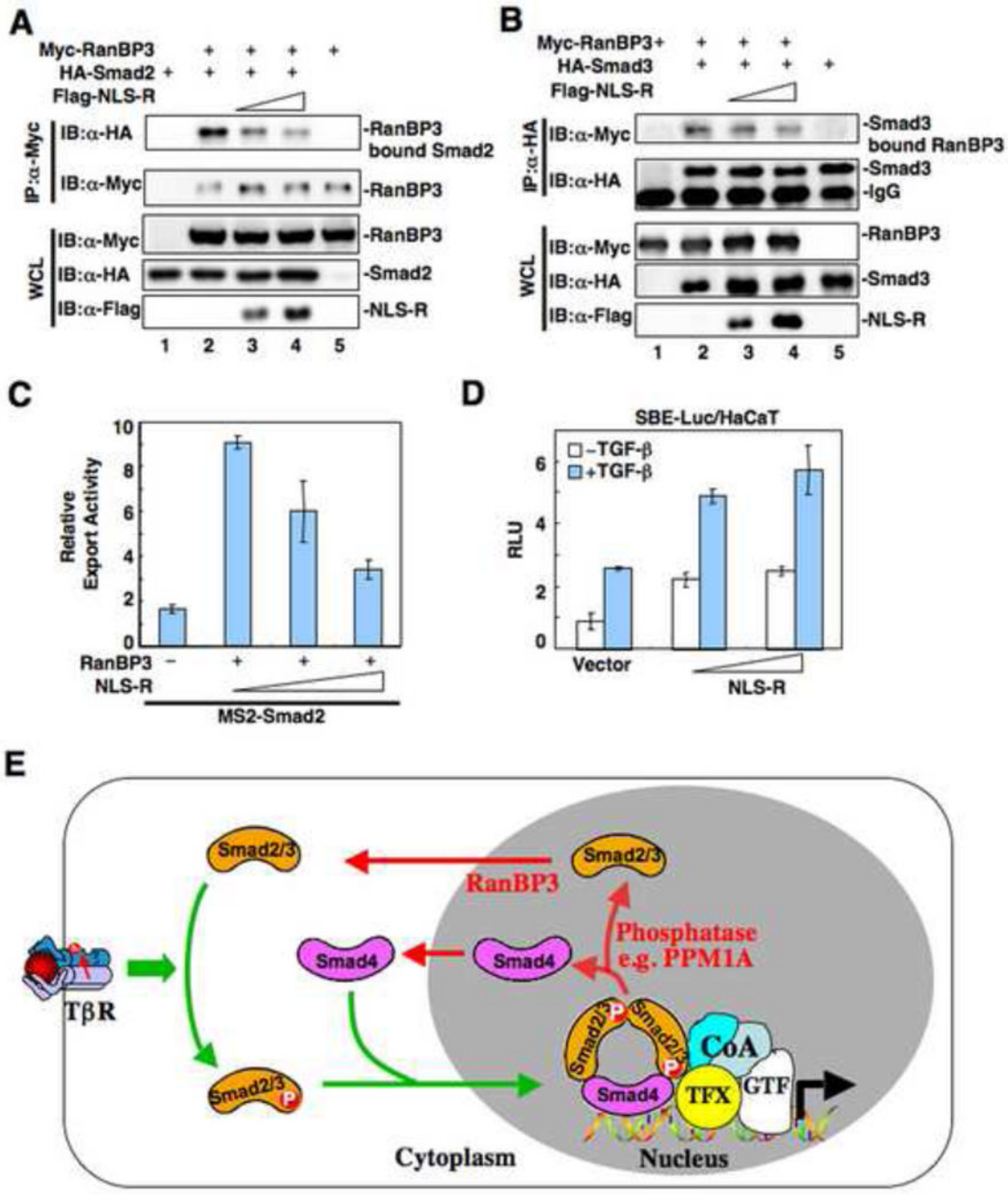

Figure 7. RanBP3 controls Smad2/3 export and TGF-β signaling via its contact with Smad2/3

(A) Effect of Flag-NLS-RanBP3-R (Flag-NLS-R) on the RanBP3-Smad2 interaction. HEK293T cells were transfected with indicated expression plasmids and co-IP experiments were carried as described in Figure 4A.

(B) Effect of Flag-NLS-R on the RanBP3-Smad3 interaction.

(C) Effect of Flag-NLS-R on RanBP3-mediated Smad2 export was examined using a quantitative Smad2 export assay. Values and error bars represent mean and standard deviation of two experiments.

(D) Effect of Flag-NLS-R on the SBE-luc reporter activity. Flag-NLS-R was co-transfected into HaCaT cells, and the SBE-Luc reporter activity was measured 20 h after TGF-β stimulation.

(E) A working model for Smad2/3 transport. During TGF-β signal transduction (indicated by green arrows), receptor-phosphorylated Smad2/3 form a complex with Smad4. The heteromeric Smad complex is then recruited to transcriptional machinery via its binding to the promoter, Smad-cooperating transcription factors (TFX) and co-activators (Co-A) such as p300/CBP, TAZ and the Mediator complex. During signal termination (red arrows), Smad2/3 become dissociated and dephosphorylated by PPM1A. Dephosphorylated Smad2/3 is then exported out of the nucleus by RanBP3 in a Ran-dependent manner. Signal transduction may be re-initiated, dependent on receptor activity. TβR, TGF-β receptor complex; GTF, general transcription factors.